2012

Monitoring live fuel moisture using soil moisture and remote sensing proxies

Yi Qi
University of Nebraska-Lincoln, yqi7@unl.edu

Philip E. Dennison
University of Utah

Jessica Spencer
University of Utah

David Riano
University of California, Davis

Research Article

Monitoring Live Fuel Moisture Using Soil Moisture and Remote Sensing Proxies

Yi Qi[1*], Philip E. Dennison[1], Jessica Spencer[1], and David Riaño[2,3]

[1] Department of Geography, University of Utah,
260 S. Central Campus Drive, Room 270, Salt Lake City, Utah 84112-9155, USA

[2] Center for Spatial Technologies and Remote Sensing, University of California,
One Shields Ave, 139 Veihmeyer Hall, Davis, California 95616-8617, USA

[3] Instituto de Economía y Geografía,
Centro de Ciencias Humanas y Sociales, Consejo Superior de Investigaciones Científicas,
Albasanz 26-28, Madrid 28037, Spain

[*]Corresponding author: Tel.: 001-801-581-8218; e-mail: yi.qi@utah.edu

ABSTRACT

Live fuel moisture (LFM) is an important fuel property controlling fuel ignition and fire propagation. LFM varies seasonally, and is controlled by precipitation, soil moisture, evapotranspiration, and plant physiology. LFM is typically sampled manually in the field, which leads to sparse measurements in space and time. Use of LFM proxies could reduce the need for field sampling while potentially improving spatial and temporal sampling density. This study compares soil moisture and remote sensing data to field-sampled LFM for Gambel oak (*Quercus gambelii* Nutt) and big sagebrush (*Artemisia tridentata* Nutt) in northern Utah. Bivariate linear regression models were constructed between LFM and four independent variables. Soil moisture was more strongly correlated with LFM than remote sensing measurements, and produced the lowest mean absolute error (MAE) in predicted LFM values at most of the sites. When sites were pooled, canopy water content (CWC) had stronger correlations with LFM than normalized difference vegetation index (NDVI) or normalized difference water index (NDWI). MAE values for all proxies were frequently above 20 % LFM at individual sites. Despite this relatively large error, remote sensing and soil moisture data may still be useful for improving understanding of spatial and temporal trends in LFM.

Keywords: live fuel moisture, MODIS, remote sensing, soil moisture

Citation: Qi, Y., P.E. Dennison, J. Spencer, and D. Riaño. 2012. Monitoring live fuel moisture using soil moisture and remote sensing proxies. Fire Ecology 8(3): 71-87. doi: 10.4996/fireecology.0803071

INTRODUCTION

Live fuel moisture (LFM) is an important fuel property for assessing fire danger. LFM is defined as the proportion of water content to dry matter content in live vegetation. LFM has been incorporated in fire danger rating systems, such as the National Fire Danger Rating System (NFDRS) in the US (Deeming *et al*. 1978) and the Canadian Forest Fire Danger Rating System (CFFDRS) (Stocks *et al*. 1989). LFM can also be used by fire behavior models to determine energy needed for ignition and fire spread rate (Rothermel 1972). The direct measurement of LFM is done by collecting fresh field samples, drying them until all moisture is evaporated, and calculating the water content using the mass difference between fresh and dry samples (Lawson and Hawkes 1989, Pollet and Brown 2007). Field-sampled LFM represents conditions for a vegetation species at a single site and time, but it is difficult to extrapolate field measurements to larger regions and longer time periods.

Previous studies have used meteorological indices to estimate LFM (Burgan *et al*. 1998, Viegas *et al*. 2001, Sebastián-López *et al*. 2002). Although weather data are easily accessible, two problems still challenge meteorological indices: first, meteorological indices assume a constant relationship between observed parameters and LFM; and second, meteorological data are still linked to point observations that may not be representative of larger areas. LFM is fundamentally controlled by the plant physiology and soil water availability, so meteorological indices may not reflect local variation in topography, soil type, precipitation, and vegetation type and cover. Extreme weather conditions like foehn winds can also complicate relationships between meteorological data and LFM.

Remote sensing data have been proposed for use in LFM estimation to improve spatial and temporal coverage. Most empirical studies have used band-ratio indices or radiative transfer models (RTM) to correlate variables based on vegetation greenness or moisture content with field-measured LFM. Results of previous studies have varied across study sites and species (Dennison *et al*. 2005, Roberts *et al*. 2006, Yebra *et al*. 2008). Another potential proxy for LFM, soil moisture, has not previously been compared to field-measured LFM. Our research investigates four potential proxies for LFM that could improve spatial and temporal coverage of LFM estimation. Soil moisture responds to precipitation and evapotranspiration, and soil moisture measurements can be done continuously. Remote sensing provides extensive spatial coverage with a temporal resolution similar to current LFM sampling protocols (Dennison *et al*. 2005). The objectives of this research were to: 1) examine relationships between soil moisture and LFM and determine whether soil moisture has potential as an LFM proxy, and 2) compare soil moisture to more established remote sensing indices as proxies for LFM estimation.

BACKGROUND

Seasonal LFM variation is controlled by precipitation, soil moisture, evapotranspiration, and plant physiology. Water is transported along a water potential gradient in the soil-plant-atmosphere continuum. The soil water potential generally declines with decreasing soil moisture, and corresponding plant water uptake drops due to smaller hydraulic conductance between soil and root (Schulze *et al*. 2005). Soil moisture available to vegetation is controlled by soil properties, precipitation, and evapotranspiration fluxes over time scales of weeks to years. In extreme conditions, rapid dry down can happen in days, for example during Santa Ana winds affecting southern California. The relationship between drought and fuel moisture is presumably that low precipitation or high evapotranspiration result in lower LFM and increase wildfire area burned (Keetch and Byram 1968, Bessie and Johnson 1995, Chuvieco *et al*. 2009, Littell *et al*. 2009).

LFM trends in southern California chaparral have been predicted using seasonal precipitation (Dennison *et al*. 2008) and monthly precipitation terms (Dennison and Moritz 2009). Previous studies have designed soil water indices to estimate LFM. Dimitrakopoulos and Bemmerzouk (2003) demonstrated a strong relationship between the Keetch Byram Drought Index (KBDI) (Keetch and Byram 1968) and LFM for herbaceous understory vegetation in a Mediterranean pine forest. KBDI uses precipitation and maximum temperature to estimate the net effect of daily precipitation and evapotranspiration on soil water balance. Dennison *et al.* (2003) found a strong, nonlinear relationship between a cumulative water balance index (CWBI) model and LFM in chaparral. CWBI cumulatively sums precipitation and reference evapotranspiration over time. More complex than the standard KBDI, the Dennison *et al.* (2003) CWBI calculated reference evapotranspiration from a modified Penman equation (Snyder and Pruitt 1992) using solar irradiance, air temperature, vapor pressure, and wind speed, but did not take into account plant physiology. To our knowledge, no previous study has directly compared *in situ* soil moisture measures to field-sampled LFM.

Remote sensing offers a potentially cost-effective way to improve LFM temporal and spatial monitoring. The reflectance spectrum of vegetation contains absorption features that result from harmonics and overtones of various foliar chemical components (Curran 1989). At the leaf level, the typical spectral features of green vegetation include chlorophyll absorption in the visible (400 nm to 700 nm), leaf structure expressed in the near infrared (NIR, 700 nm to 1300 nm), and water absorption dominating in the shortwave infrared (SWIR, 1300 nm to 2500 nm) (Ceccato *et al*. 2001, Bowyer and Danson 2004). At the canopy level, reflectance is a function of solar and view geometry, leaf-level reflectance, canopy structure, and vegetation cover. As LFM declines, visible and SWIR reflectance generally increase while NIR reflectance decreases (Figure 1). Changes in NIR reflectance and water absorption with changing LFM can be used to predict LFM from remote sensing data (Chuvieco *et al*. 2002, Dennison *et al*. 2005). Changes in indices measuring chlorophyll absorption have also been correlated with changes in LFM (Roberts *et al*. 2006, Stow *et al*. 2006), since vegetation greenness measures have shown good correlation with moisture content in ecosystems such as grasslands and shrublands.

Remote sensing data have been proven useful for estimating LFM using empirical methods and radiative transfer models (RTM) (Chuvieco *et al*. 2009). Most empirical studies have used regression analyses to compare vegetation indices with field-measured LFM (e.g., Dennison *et al*. 2005, Roberts *et al*. 2006, Stow *et al*. 2006). RTM simulates the reflectance, absorption, and transmission of electromagnetic radiation at leaf and canopy scales and has been mathematically inverted to estimate canopy water content and LFM (Zarco-Tejada 2003, Riaño *et al*. 2005; Trombetti *et al*. 2008, Yebra and Chuvieco 2009). Many previous papers have focused on Mediterranean vegetation, such as chaparral in southern California (Ustin *et al*. 1998, Serrano *et al*. 2000, Dennison *et al*. 2005, Roberts *et al*. 2006), and herbaceous vegetation and shrubland in Spain (Chuvieco *et al*. 2003, 2004). Yebra *et al*. (2008) found that empirical and RTM methods had comparable performance for LFM estimation in Mediterranean vegetation, but RTM was more robust for applications across different species and sites.

METHODS

We conducted this research at ten sites in northern Utah, USA (Table 1). Two species, Gambel oak (*Quercus gambelii* Nutt) and big sagebrush (*Artemisia tridentata* Nutt) were studied at five sites each. These sites were chosen because they were operational LFM

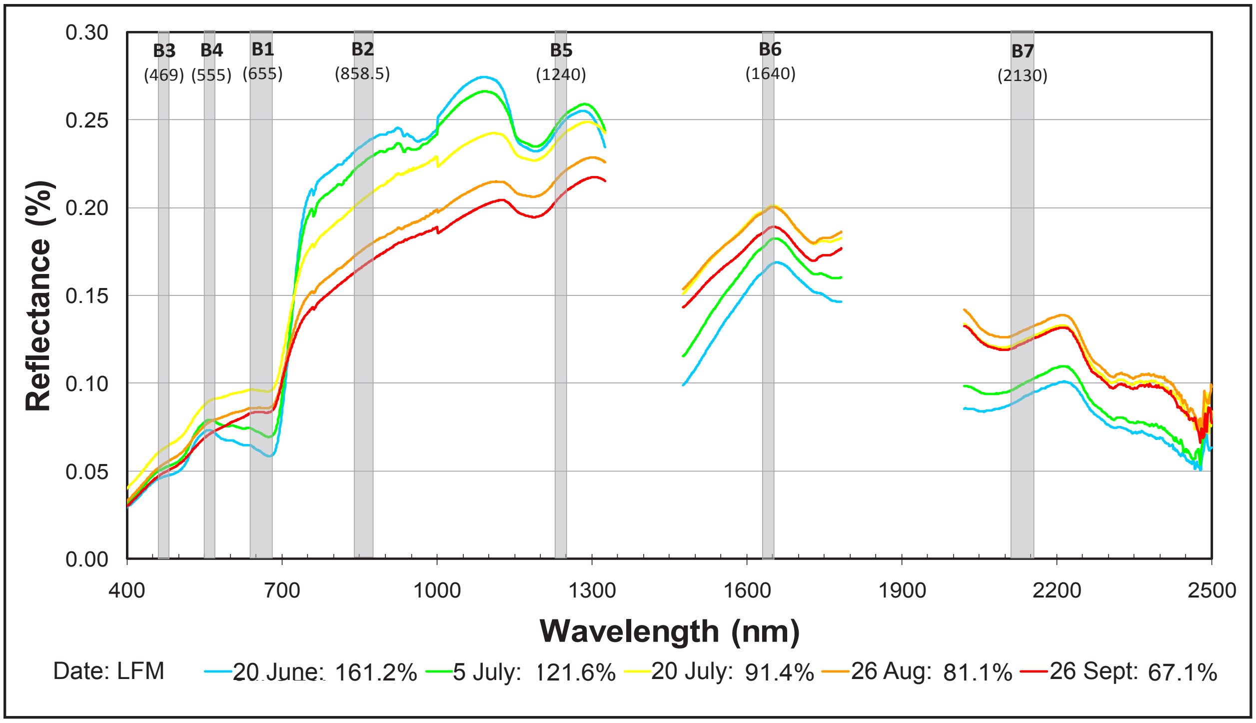

Figure 1. An example of field reflectance spectra (400 nm to 2500 nm) for sagebrush collected over the summer of 2005 near the Vernon site. As the line colors change from blue to red, LFM decreases. MODIS bands (grey) with their central wavelengths (in parentheses) are also shown.

field sampling sites for the US Bureau of Land Management (BLM) or Forest Service (USFS). The sites were within a geographic region approximately 8800 km^2 in size, and covered large gradients in elevation (1582 m to 2073 m), slope (2 degrees to 33 degrees), vegetation cover, and meteorological conditions.

Field-sampled LFM data were downloaded from the National Fuel Moisture Database (NFMD: http://72.32.186.224/nfmd/public/index.php, last accessed November 2012). Standard protocols for LFM sampling established by Pollet and Brown (2007) were followed by BLM and USFS personnel. Live foliage and pliable small stem material (up to 0.32 cm [1/8 inch] diameter) were clipped from Gambel oak and sagebrush shrubs. Several shrubs were sampled at different heights and aspects. Samples were stored in containers with tight-fitting lids and kept cool and dry. The samples were weighed in the field to provide wet mass, and then were dried in a mechanical convection oven for at least 24 hours at 100 ^{o}C and reweighed to provide dry mass. LFM was calculated by dividing the water mass (wet mass – dry mass) by the dry mass. LFM was generally sampled bi-weekly during the summer and fall, and species names, sampling dates, and LFM values were submitted to the NFMD. Plant phenology is known to affect LFM, since samples are typically collected without regard for leaf age.

In the summers of 2009 and 2010, soil moisture stations were installed at LFM sampling locations in collaboration with BLM and USFS personnel. At each site, a 15 cm (6 inch) diameter hole was dug and four Decagon 5TE probes were inserted into the hole wall. Rocky soils prevented deep probe placement at many of the sites, so probes were placed at all sites as follows: two at a depth of 20 cm, and two at 40 cm. Volumetric soil water content (m^3 m^{-3}) and soil temperature (^{o}C) were recorded by a Decagon Em50 data logger every 60 min.

Table 1. Description of ten study sites in northern Utah, USA, including geographic locations, species, soil texture at 20 cm depth, slope, aspect (in degrees from north), elevation, soil moisture measurement start date, number of LFM observations, and maximum and minimum of LFM measurements.

Site	Lat	Long	Species	Soil Texture	Slope (º)	Aspect (º)	Elevation (m)	Start Date	*n*	LFM (%)	
										Max	Min
Little Cottonwood	40.57	–111.77	Gambel oak	Loamy sand	15	208	1718	18/5/09	26	191	79
Hobble Creek	40.15	–111.54	Gambel oak	Sandy loam	33	202	1910	6/6/10	14	217	76
Maple Canyon	40.13	–111.53	Gambel oak	Sandy loam	29	162	1870	6/6/10	16	201	79
Squaw Peak	40.30	–111.62	Gambel oak	Clay	8	50	2073	8/6/10	12	152	81
Black Cedar	38.98	–112.24	Gambel oak	Clay loam	6	285	1979	7/6/10	20	231	89
Vernon	40.06	–112.33	big sagebrush	Gravelly loam	2	35	1712	28/4/09	59	237	57
Mud Springs	39.88	–112.22	big sagebrush	Sandy loam	6	18	1790	5/5/09	38	221	67
Muskrat	40.64	–112.65	big sagebrush	Very gravelly loam	16	259	1582	3/6/10	36	210	63
Sevier Reservoir	39.33	–112.06	big sagebrush	Sandy loam	9	44	1662	7/6/10	22	197	71
Black Cedar	38.98	–112.24	big sagebrush	Clay	6	285	1979	7/6/10	22	230	78

Measurements over 24 hr periods were averaged to provide daily soil moisture values. Since incomplete contact with the soil can result in low measured soil moisture, the probe with the highest average moisture at the 20 cm depth was used for further analysis. Incomplete data were available for the Black Cedar Gambel oak site after the data logger was accidentally disconnected from the probes, likely due to disturbance by grazing cattle.

The Terra Moderate Resolution Imaging Spectroradiometer (MODIS) surface reflectance product MOD09A1 was used to calculate remote sensing measures. MOD09A1 is an 8-day composite product of atmospherically corrected reflectance for the first seven spectral bands of the MODIS instrument at 500 meter spatial resolution (bands shown in Figure 1). The original products were downloaded from the Oak Ridge National Laboratory MODIS Global Subsets site (http://daac.ornl.gov/cgi-bin/MODIS/GLBVIZ_1_Glb/modis_subset_order_global_col5.pl, revised 7 March 2012, last accessed November 2012). Cloud and bad band data were masked using a MODIS quality assurance layer. The 500 m pixel containing each soil moisture or LFM sampling site was extracted and three remote-sensing based measures were calculated from MODIS bands: normalized difference vegetation index (NDVI), normalized difference water index (NDWI), and canopy water content (CWC). NDVI is a normalized ratio between NIR and red reflectance (Rouse *et al*. 1973) that captures both chlorophyll absorption in the visible and leaf additive reflectance in the NIR spectral region:

$$\frac{\rho_{856} - \rho_{655}}{\rho_{856} + \rho_{655}} \,, \tag{1}$$

where the subscript indicates the band center wavelength in nanometers. Higher NDVI values indicate higher chlorophyll absorption, leaf area, and vegetation cover. NDWI is a normalized ratio between a NIR band and a SWIR band that can be used for estimating vegetation liquid water content (Gao 1996):

$$\frac{\rho_{856} - \rho_{1240}}{\rho_{856} + \rho_{1240}} \,. \tag{2}$$

NDVI and NDWI have shown strong correlations with LFM in previous studies (Roberts *et al*. 2006; Stow *et al*. 2006). CWC was calculated by an inversion of a radiative transfer model through an artificial neural network (ANN) (Trombetti *et al*. 2008) combined with NDVI and normalized difference indices using 1640 nm and 2130 nm as absorption bands. The Prospect-SailH radiative transfer model (Jacquemoud *et al*. 1995; Kuusk 1995) was used by Trombetti *et al*. (2008) to derive CWC. The CWC (expressed in mm) was computed as the product of leaf area index and leaf water content, which was defined as the theoretical thickness of a single layer of water per unit leaf area. Modeled CWC is not equivalent to LFM, since LFM is dependent on the amount of dry matter in relation to CWC. However, if dry matter remains relatively stable over time, then CWC and LFM should be strongly correlated.

For each site, we conducted regression analyses between LFM and each independent variable, including soil moisture, CWC, NDVI, and NDWI. Coefficient of determination (R^2) values of the four bivariate linear regression models were calculated to investigate performance of soil moisture and remote sensing proxies in explaining LFM variation. We calculated the mean absolute error (MAE) for each regression model to measure the average magnitude of LFM estimation errors. To test the model performance across sites and species, we applied regression models to pooled datasets among and between species. LFM variation is dependent on local characteristics of individual sites. To eliminate cross-site diversity within the pooled data, an offset was calculated for each proxy as its value subtracted by its mean value for that site, then these offsets were pooled together from all sites. Bootstrap validation was employed to test the robustness of each model for the pooled data. For each explanatory parameter, a random number of observations were taken out with replacement from the samples, and a new linear regression model was constructed. We then calculated the R^2, calibration error (root mean square error of residuals between predicted and observed LFM of all observations), and validation error (root mean square error of residuals between predicted and observed LFM of taken-out observations) of the new model. The bootstrap validation was repeated 1000 times to examine the model robustness.

RESULTS

Time series of LFM demonstrated seasonal patterns of green-up in early spring and drying down through late spring and summer. The amplitude and timing of seasonal changes varied considerably between years. An example is provided by the Vernon big sagebrush site (Figure 2). Big sagebrush LFM measurements started at 200 % LFM at day 110 in 2010 and 154 % LFM at day 103 in 2011. LFM peaked and decreased earlier in 2010 than 2011. Both years showed similar LFM in late summer and a slight increase in LFM in the fall, but this happened about 15 days earlier in 2011. All proxies generally decreased at different rates. In 2011, soil moisture spiked and then gradually declined in spring due to precipitation events.

Strength of correlations between LFM and the four independent variables varied across sites (Table 2). Soil moisture showed positive relationships with LFM and the highest R^2 value (0.66) when averaged across all ten sites. The R^2 values for soil moisture were generally higher than those for remote sensing variables,

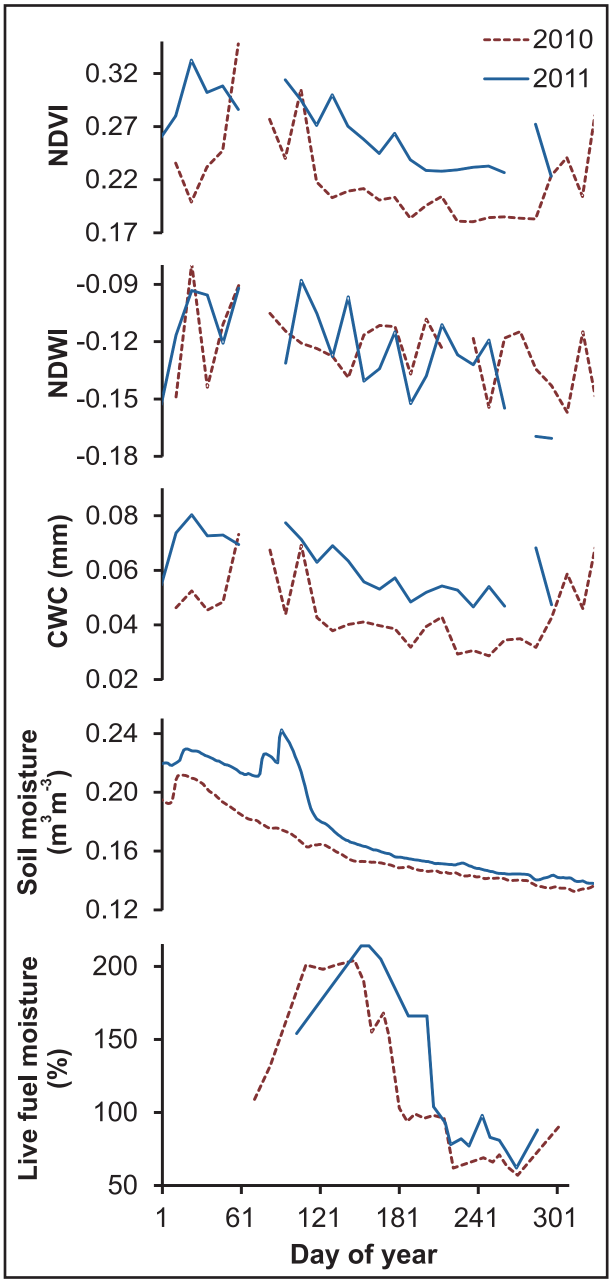

Figure 2. 2010 and 2011 time series plots for the Vernon big sagebrush site. Some remote sensing measures are missing following removal by quality assessment.

with the exception of big sagebrush sites at Mud Springs and Muskrat. Values of R^2 for soil moisture were also more stable across sites. The weakest relationship for soil moisture was for big sagebrush at the Muskrat site, with an R^2 value of 0.41. The strongest relationship for soil moisture was Gambel oak at the Squaw Peak site, where the R^2 of the relationship with LFM was 0.89. Mean of MAE across all sites was lowest for soil moisture, with a mean MAE of 17.1% LFM. The smallest MAE was 5.14% at the Squaw Peak Gambel oak site, while the largest MAE was 28.79% for big sagebrush at Mud Springs. For species averages, Gambel oak showed higher R^2 and smaller MAE than big sagebrush.

Among the remote sensing measures, each regression model showed wide variation within sites of same species and between species (Figures 3 and 4). The highest R^2 values for each variable were found at Squaw Peak with CWC (0.7), Muskrat with NDVI (0.75), and Squaw Peak with NDWI (0.69). All remote sensing measures had smaller averaged R^2 values than soil moisture, and multiple measures had weak correlations with LFM ($R^2 < 0.2$) at Maple Canyon and Black Cedar. NDVI had stronger correlations than CWC and NDWI at six sites, and NDVI had a slightly higher averaged R^2 of 0.35. Comparing the two species, CWC and NDVI showed stronger correlations with big sagebrush, but NDWI had a higher averaged R^2 with Gambel oak. MAE results also varied across sites and proxies within a range between 8.6% LFM and 34% LFM. Mean MAE values were 22.3% for NDVI, 22.9% for CWC, and 25.6% for NDWI. Soil moisture had smaller MAE values than the remote sensing proxies at all five Gambel oak sites and two big sagebrush sites except Mud Springs and Muskrat. Gambel oak had smaller averaged MAE values for remote sensing variables than big sagebrush. Some soil moisture values diverged from the general trends, for example in the big sagebrush sites Vernon (Figure 4d) and Muskrat (Figure 4i). According to the historical weather and soil moisture data, many abnormally high soil moisture values were observed following precipitation events. Soil moisture was higher in the short-term, while LFM changed more slowly with a peak that lagged peak soil moisture (Figure 2).

Table 2. R^2 and mean absolute error (MAE) of bivariate linear regression results between LFM and soil moisture or remote sensing variables. N/A: No analysis due to bovine disturbance of soil moisture data logger. Significance levels: *** $P < 0.001$, ** $P < 0.01$, * $P < 0.05$.

	CWC		NDVI		NDWI		Soil moisture	
Site	**R^2**	**MAE**	**R^2**	**MAE**	**R^2**	**MAE**	**R^2**	**MAE**
Little Cottonwood	0.38^{**}	17.66	0.13	21.98	0.22^{*}	21.65	0.63^{***}	14.15
Hobble Creek	0.36^{*}	20.12	0.4^{*}	18.35	0.24	24.13	0.86^{***}	9.76
Maple Canyon	0.12	21.77	0.01	24.36	0.38^{*}	18.09	0.86^{***}	10.72
Squaw Peak	0.7^{***}	8.63	0.58^{**}	9.61	0.69^{***}	9.77	0.89^{***}	5.14
Black Cedar	0.01	26.59	018	25.61	0.06	28.1	0.53^{***}	18.45
Vernon	0.34^{***}	33.49	0.39^{***}	31.81	0.38^{***}	33.98	0.65^{***}	24.51
Mud Springs	0.6^{***}	22.39	0.62^{***}	22.36	0.46^{***}	27.59	0.46^{***}	28.79
Muskrat	0.39^{***}	25.35	0.75^{***}	15.44	0.22^{**}	31.61	0.41^{***}	22.87
Sevier Reservoir	0.45^{***}	20.06	0.46^{***}	19.7	0.24^{*}	26.95	0.63^{***}	19.52
Black Cedar	0.02	34.09	0.01	34.05	0.02	34.05	N/A	N/A
Average of Gambel oak	0.32	18.69	0.26	19.98	0.32	20.35	0.75	11.64
Average of big sagebrush	0.36	27.07	0.44	24.67	0.26	30.84	0.54	23.92
Average of all sites	0.34	22.88	0.35	22.33	0.29	25.59	0.66	17.1
Pooled Gambel oak	0.13^{***}	19.74	0.01	22.29	0.12^{***}	20.97	0.65^{***}	13.31
Pooled big sagebrush	0.31^{***}	31.52	0.26^{***}	32.68	0.24^{***}	34.08	0.48^{***}	20.04
Pooled all sites	0.27^{***}	28.05	0.15^{***}	31.45	0.18^{***}	31.53	0.49^{***}	23.97

In the regression models for pooled datasets, soil moisture showed the strongest correlation with an R^2 of 0.65 for Gambel oak, 0.48 for big sagebrush, and 0.49 for all sites (Figure 5). Across all sites and across individual species, CWC had a higher pooled R^2 than NDVI and NDWI. For remote sensing measures, big sagebrush had higher pooled R^2 values. Soil moisture had smaller MAE than other proxies, and Gambel oak sites had smaller MAE than big sagebrush sites (Table 2). Boxplots shown in Figure 6 demonstrate the range of R^2 values, calibration errors, and validation errors from bootstrap validation. Soil moisture showed a median R^2 of 0.5 across all sites, followed by CWC, NDWI, and NDVI. Soil moisture also

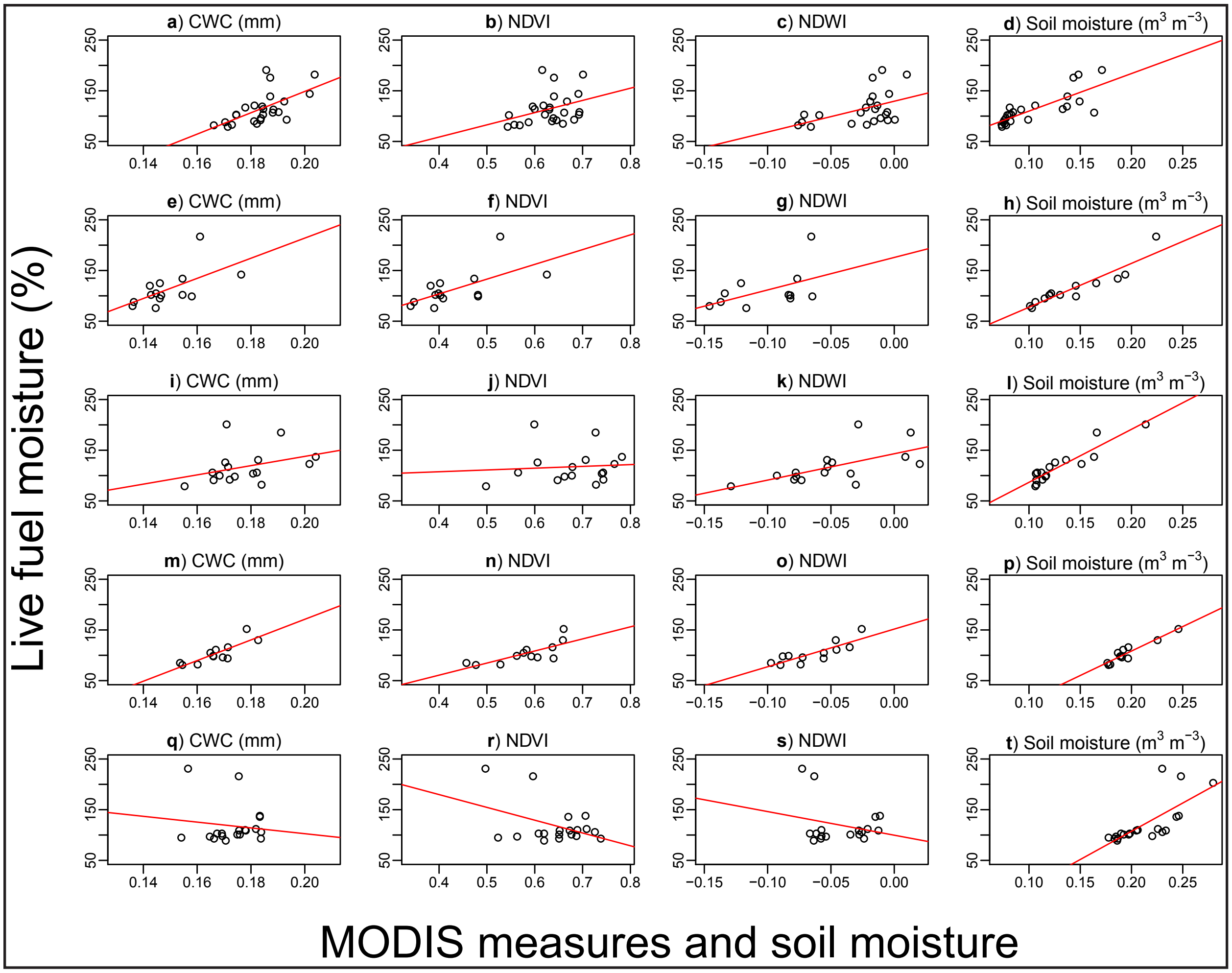

Figure 3. Plots of MODIS-derived CWC, NDVI, NDWI, and soil moisture against LFM for Gambel oak sites: Little Cottonwood Canyon (a to d), Hobble Creek (e to h), Maple Canyon (i to l), Squaw Peak (m to p), and Black Cedar (q to t). The red lines indicate best fit linear equations.

had the smallest calibration error and validation error. The stronger correlations with soil moisture were maintained for both species. The three remote sensing proxies had higher R^2 for big sagebrush than Gambel oak. CWC showed consistently better performance than the two indices. NDVI had stronger correlations than NDWI only for big sagebrush. The calibration errors and validation errors for big sagebrush were generally larger than those for Gambel oak.

DISCUSSION

The regression models and bootstrap validation demonstrated that soil moisture was most strongly correlated with LFM in both species and across sites. The median R^2 of validation showed that about 50 % LFM variation was explained by soil moisture in the pooled data. The unexplained variation might be partially related to soil depth, soil available water capacity, and plant physiology. The soil available water capacity, the water content between field capacity and wilting point, is determined by soil texture. Some Gambel oak sites had fine soil texture, like clay loam at Black Cedar and clay at Squaw Peak. However, big sagebrush sites had coarse soil texture including sandy loam and gravelly loam (Table 1). Fine soil with narrow pore spacing can hold more water than coarse soils with wide pore

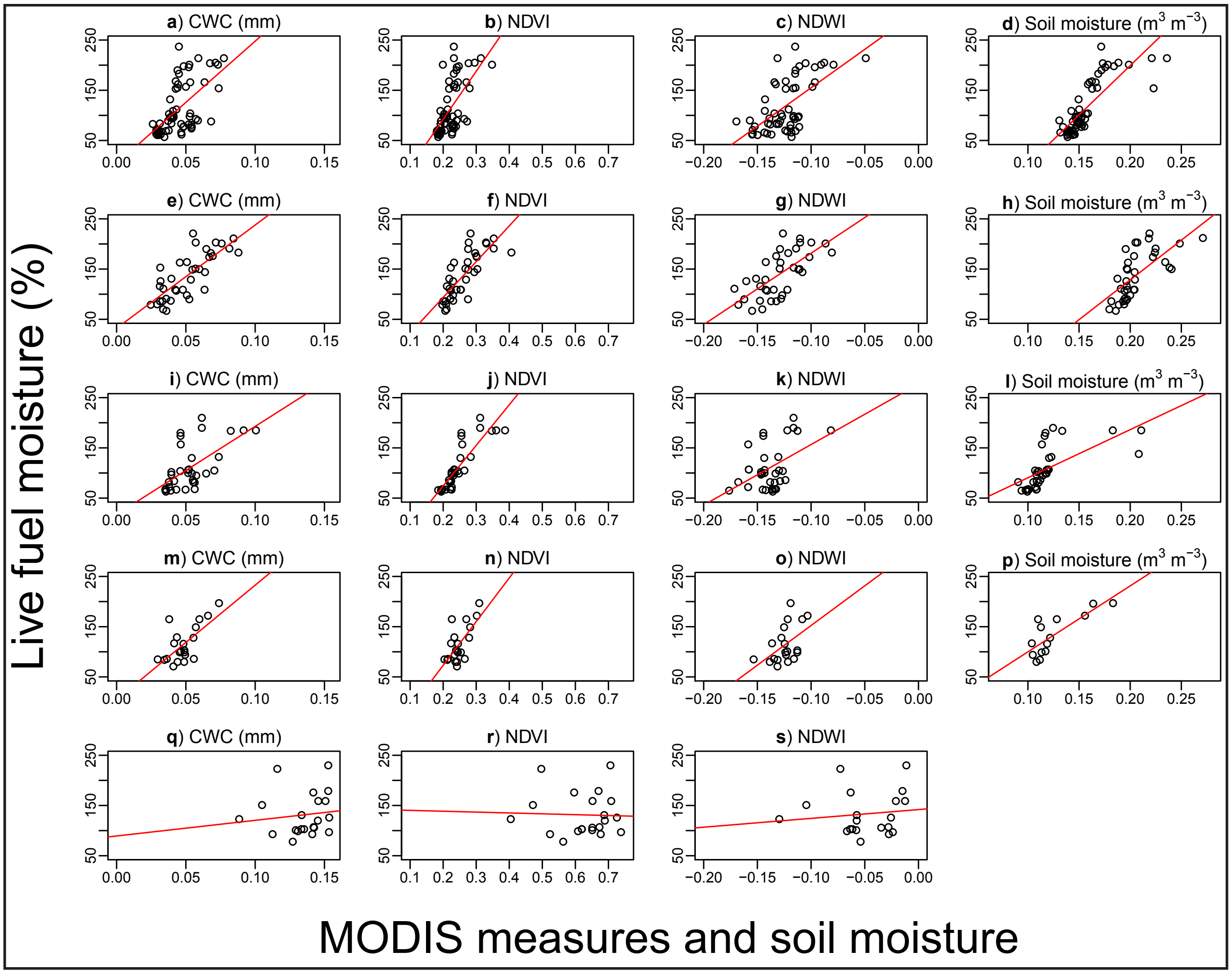

Figure 4. Plots of MODIS-derived CWC, NDVI, NDWI, and soil moisture against LFM for big sagebrush sites: Vernon (a to d), Mud Spring (e to h), Muskrat (i to l), Sevier Reservoir (m to p), and Black Cedar (q to s). The red lines indicate best fit linear equations.

spacing. Given the same meteorological conditions, soil at Gambel oak sites might provide more available water to support plants than soil at big sagebrush sites. We did not have soil depth data for our sites. The minimum root depth of big sagebrush is 40 cm, and Gambel oak is 91 cm (USDA Plants Database: http://plants.usda.gov/java/, last accessed November 2012). Both species have a deep taproot coupled with laterally diffused roots near the surface, allowing plants to absorb water from both surface precipitation and the water table several meters beneath. In addition, soil moisture may increase rapidly due to precipitation recharge, while LFM exhibits a lagged response.

The spatial variability of soil moisture can be influenced by small scale factors such as soil type, topography, and vegetation species, and large scale factors such as variability in precipitation and evapotranspiration (Entin *et al*. 2000, Brocca *et al*. 2007). A single soil moisture station at each site cannot capture local spatial variation in soil moisture. Some of our sites were on steeper slopes, where the local hydraulic drainage conditions were different from flat sites. This might partially cause the wide variation of R^2 values among sites. In addition, big sagebrush has high tolerance to drought and restricted water conditions (Kolb and Sperry 1999), and is thus less vulnerable to soil moisture variation than Gambel oak. At

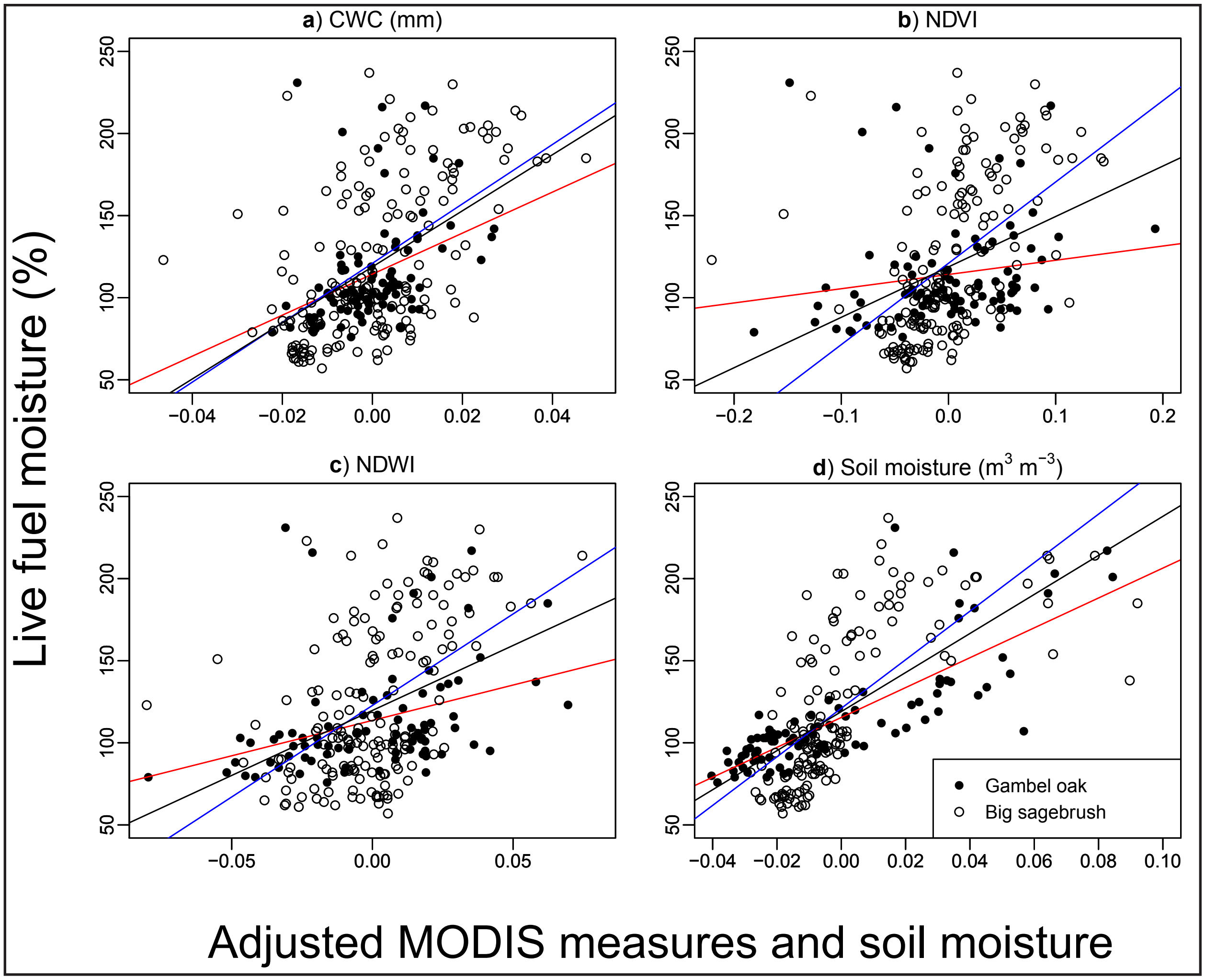

Figure 5. Plots of soil moisture and MODIS-derived CWC, NDVI, and NDWI after offset adjustment and pooling for all 10 sites. Black circles correspond to Gambel oak, and open circles correspond to big sagebrush. Blue lines correspond to linear fits to big sagebrush data; red lines correspond to linear fits to Gambel oak data; and black lines correspond to linear fits to all data.

larger scales, our ten sites covered a geographical region in northern Utah with varied topography, ecosystem, and weather conditions. As a result, pooling data across multiple years and sites incorporated different seasonality and inter-annual variation into the regression models, which partially contributed to small R^2 and large MAE for some sites and pooled data across species.

Among the three remote sensing proxies, CWC showed the best regression results with higher R^2 in the pooled data and smaller validation errors. This demonstrates the comparative advantages of using RTM across sites and species rather than relying on band-ratio indices. Between the two indices, NDVI showed slightly better explanatory performance than NDWI for big sagebrush sites and pooled data, but NDVI had weak correlation with LFM for Gambel oak sites. There are several potential factors that could influence the strength of correlations between LFM and remote sensing measurements. Although MODIS data had been screened by a quality assurance layer to eliminate bad data before building models, error in atmospheric correction and geometric

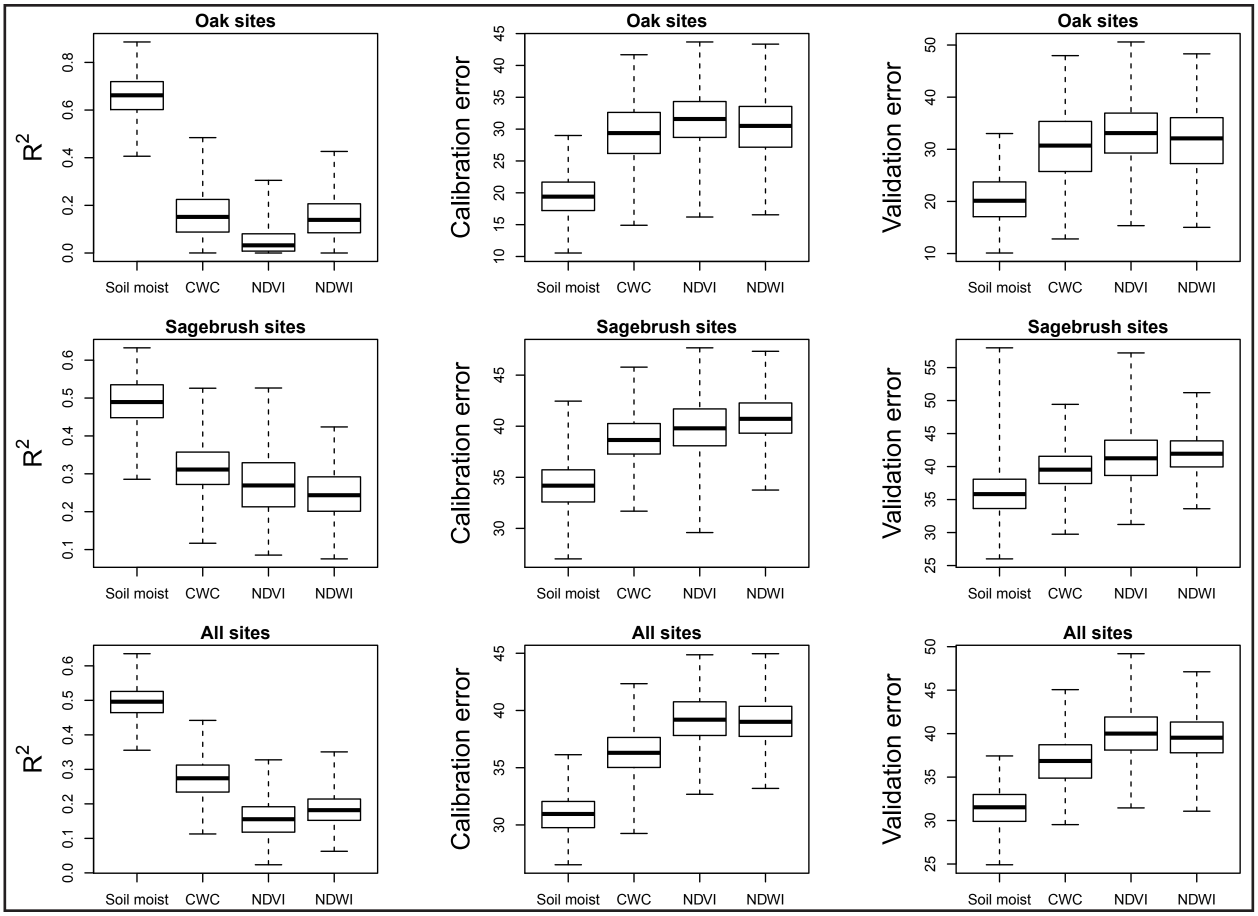

Figure 6. Boxplots of bootstrap validation for R^2 (left column), calibration error (middle column), and validation error (right column) for Gambel oak (top row), big sagebrush (middle row), and all sites (bottom row). The bottom and top ends of the whiskers represent the minimum and maximum. The bottom and top of each box represent the first and third quartiles. The band near the middle of each box represents the median.

errors may be present in MODIS data (Vermote and Kotchenova 2008). Fensholt *et al.* (2010) showed that MODIS red and NIR reflectance were highly dependent on sun-sensor geometry, and NDVI variation was dependent on vegetation density. The MOD09A1 data were not corrected by bidirectional reflectance distribution function (BRDF) to near-nadir reflectance. Both NDVI and NDWI use MODIS band 2 (NIR), so they could be affected by seasonal and inter-annual variation in viewing geometry (Sims *et al*. 2011).

An important underlying assumption of upscaling LFM field sampling to a remote sensing pixel is that remote sensing data are exclusively sensitive to changes in LFM. In fact, the surface reflectance was an aggregated product of radiative interaction with all features on the landscape within a ground instantaneous field of view (GIFOV). The radiance measured within a MODIS GIFOV is assigned to a 500 m pixel, but can in fact be a measurement of a much larger area depending on viewing geometry. Due to changes in viewing geometry over an orbital cycle, the area measured by a single pixel may not be consistent over time. Even within a single 500 m by 500 m area, vegetation can be spatially heterogeneous. Many of the ten sites had multiple vegetation species and complex topography and land cover within a 500 m radius of the site. Changes in features other than the targeted fuel type introduced spectral variation in surface reflectance and challenged successful linkage between LFM and each remote sensing variable. For instance, the mixed landscape of big sagebrush, Gambel oak, and exposed soil at the Black Cedar sites might explain the oddly negative slopes and weak correlations with remote sensing proxies (Figures 3q-s and 4q-s).

A final complicating factor for the remote sensing measures is that NDVI, NDWI, and CWC are indirectly related to LFM. NDVI is more closely related to chlorophyll than water content. Variation in chlorophyll content can be caused not only by moisture content, but also by plant nutrient deficiency, disease, and phenological stages (Ceccato *et al*. 2002, Bowyer and Danson 2004). NDWI and CWC have stronger connections to water content but do not explain dry matter variation that is a part of the LFM equation (Serrano *et al*. 2000). CWC was computed by the method developed by Trombetti *et al*. (2008). The ANN inversion algorithm used by Trombetti *et al.* (2008) grouped vegetation into shrubland, forest, and grassland classes. This simplified classification might not describe landscape diversity in our sites.

Most major changes in LFM are associated with physiological activities of vegetation in response to metrological conditions and phenology. Big sagebrush starts leaf and stem growth in the spring when temperatures are warm and soil moisture is high. Growth will continue until the weather is too hot or soil moisture becomes too low to support transpiration. If moderate temperate and precipitation are present in late summer or early fall, sagebrush may produce a second flush of new growth, although at a smaller scale compared to spring. The surge of LFM in the spring, decline during the summer, and possible increase in the fall is dependent on the timing and amplitude of moisture availability. Under water stress, sagebrush will express morphological plasticity, including shedding spring leaves; allocating more biomass to vegetative versus reproductive shoots, leaves versus stems, and perennial versus ephemeral leaves. In contrast, new growth of Gambel oak generally starts in late spring and continues until late summer or early fall when soil moisture is a limiting factor. Variation in plant phenology and adaption to moisture availability needs to be accounted for at all levels, from LFM sampling through remote measurement.

CONCLUSIONS

This study examined using soil moisture and remote sensing proxies for estimating LFM in big sagebrush and Gambel oak. Soil moisture is a point-based, continuous measurement of drought condition *in situ*. Our results demonstrated that soil moisture can provide better predictive power than remote sensing measures across multiple sites and two species. It can potentially provide an alternative means for LFM estimation with more frequent temporal coverage, and a soil moisture network could complement LFM field sampling. Microwave remote sensing techniques could potentially improve spatial coverage of soil moisture monitoring (Dubois *et al*. 1995, Le Hégarat-Mascle *et al*. 2002, Njoku *et al*. 2003, Zribi *et al*. 2005), although active and passive microwave remote sensing can only retrieve near-surface soil moisture (Njoku and Entekhabi 1996, Barrett et al. 2009). Remote sensing measures proved to be less strongly correlated with LFM data, but provided superior spatial coverage. To make the remote sensing proxies more accurate for operational management, selection of high quality MODIS data with BRDF correction and more homogeneous sampling sites may improve relationships. Seasonality and inter-annual variation need to be considered in generalized models of pooled data.

ACKNOWLEDGMENTS

This research was supported by research funding from the US Department of Interior Bureau of Land Management and from NASA grant #NNX11AF93G. We would like to thank Ed Delgado and Scott Matheson for their assistance in this research. We also would like to thank the reviewers for their constructive comments.

LITERATURE CITED

Barrett, B., E. Dwyer, and P. Whelan. 2009. Soil moisture retrieval from active spaceborne microwave observations: an evaluation of current techniques. Remote Sensing 1: 210-242. doi: 10.3390/rs1030210

Bessie, W.C., and E.A. Johnson. 1995. The relative importance of fuels and weather on fire behavior in subalpine forests. Ecology 76: 747-762. doi: 10.2307/1939341

Bowyer, P., and F. Danson. 2004. Sensitivity of spectral reflectance to variation in live fuel moisture content at leaf and canopy level. Remote Sensing of Environment 92: 297-308. doi: 10.1016/j.rse.2004.05.020

Brocca, L., R. Morbidelli, F. Melone, and T. Moramarco. 2007. Soil moisture spatial variability in experimental areas of central Italy. Journal of Hydrology 333: 356-373. doi: 10.1016/j.jhydrol.2006.09.004

Burgan, R.E., R.W. Klaver, and J.M. Klaver. 1998. Fuel models and fire potential from satellite and surface observations. International Journal of Wildland Fire 8: 159-170. doi: 10.1071/WF9980159

Ceccato, P., S. Flasse, S. Tarantola, S. Jacquemoud, and J.-M. Grégoire. 2001. Detecting vegetation leaf water content using reflectance in the optical domain. Remote Sensing of Environment 77: 22-33. doi: 10.1016/S0034-4257(01)00191-2

Ceccato, P., N. Gobron, S. Flasse, B. Pinty, and S. Tarantola. 2002. Designing a spectral index to estimate vegetation water content from remote sensing data: part 1: theoretical approach. Remote Sensing of Environment 82: 188-197. doi: 10.1016/S0034-4257(02)00037-8

Chuvieco, E., D. Cocero, D. Riaño, P. Martin, J. Martínez-Vega, J. De La Riva, and F. Pérez. 2004. Combining NDVI and surface temperature for the estimation of live fuel moisture content in forest fire danger rating. Remote Sensing of Environment 92: 322-331. doi: 10.1016/j.rse.2004.01.019

Chuvieco, E., D. Riaño, I. Aguado, and D. Cocero. 2002. Estimation of fuel moisture content from multitemporal analysis of Landsat Thematic Mapper reflectance data: applications in fire danger assessment. International Journal of Remote Sensing 23: 2145-2162. doi: 10.1080/01431160110069818

Chuvieco, E., I. Aguado, D. Cocero, and D. Riaño. 2003. Design of an empirical index to estimate fuel moisture content from NOAA-AVHRR images in forest fire danger studies. International Journal of Remote Sensing 24: 1621-1637.

Chuvieco, E., I. González, F. Verdú, I. Aguado, and M. Yebra. 2009. Prediction of fire occurrence from live fuel moisture content measurements in a Mediterranean ecosystem. International Journal of Wildland Fire 18: 430-441. doi: 10.1071/WF08020

Chuvieco, E., J. van Wagtendonk, D. Riaño, M. Yebra, and S.L. Ustin. 2009. Estimation of fuel conditions for fire danger assessment. Pages 83-96 in: E. Chuvieco, editor. Earth observation of wildland fires in Mediterranean ecosystems. Springer, New York, New York, USA. doi: 10.1007/978-3-642-01754-4_7

Curran, P.J. 1989. Remote sensing of foliar chemistry. Remote Sensing of Environment 30: 271-278. doi: 10.1016/0034-4257(89)90069-2

Deeming, J.E., R.E. Burgan, and J.D. Cohen. 1978. The national fire-danger rating system—1978. USDA Forest Service General Technical Report INT-39. Intermountain Forest and Range Experiment Station, Ogden, Utah, USA.

Dennison, P.E., D.A. Roberts, S.H. Peterson, and J. Rechel. 2005. Use of Normalized Difference Water Index for monitoring live fuel moisture. International Journal of Remote Sensing 26: 1035-1042. doi: 10.1080/01431160420002739998

Dennison, P.E., D.A. Roberts, S.R. Thorgusen, J.C. Regelbrugge, D. Weise, and C. Lee. 2003. Modeling seasonal changes in live fuel moisture and equivalent water thickness using a cumulative water balance index. Remote Sensing of Environment 88: 442-452. doi: 10.1016/j.rse.2003.08.015

Dennison, P.E., and M.A. Moritz. 2009. Critical live fuel moisture in chaparral ecosystems: a threshold for fire activity and its relationship to antecedent precipitation. International Journal of Wildland Fire 18: 1021-1027. doi: 10.1071/WF08055

Dennison, P.E., M.A. Moritz, and R.S. Taylor. 2008. Evaluating predictive models of critical live fuel moisture in the Santa Monica Mountains, California. International Journal of Wildland Fire 17: 18-27. doi: 10.1071/WF07017

Dimitrakopoulos, A.P., and A.M. Bemmerzouk. 2003. Predicting live herbaceous moisture content from a seasonal drought index. International Journal of Biometeorology 47: 73-79.

Dubois, P.C., J. van Zyl, and T. Engman. 1995. Measuring soil moisture with imaging radars. IEEE Transactions on Geoscience and Remote Sensing 33: 915-926. doi: 10.1109/36.406677

Entin, J.K., A. Robock, K.Y. Vinnikov, S.E. Hollinger, S. Liu, and A. Namkai. 2000. Temporal and spatial scales of observed soil moisture variations in the extratropics. Journal of Geophysical Research 105: 865-877. doi: 10.1029/2000JD900051

Fensholt, R., I. Sandholt, S.R. Proud, S. Stisen, and M.O. Rasmussen. 2010. Assessment of MODIS sun-sensor geometry variations effect on observed NDVI using MSG SEVIRI geostationary data. International Journal of Remote Sensing 31: 6163-6187. doi: 10.1080/01431160903401387

Gao, B.-C. 1996. NDWI-A normalized difference water index for remote sensing of vegetation liquid water from space. Remote Sensing of Environment 58: 257-266. doi: 10.1016/S0034-4257(96)00067-3

Jacquemoud, S., F. Baret, B. Andrieu, F.M. Danson, and K. Jaggard. 1995. Extraction of vegetation biophysical parameters by inversion of the PROSPECT+SAIL models on sugar beet canopy reflectance data. Application to TM and AVIRIS sensors. Remote Sensing of Environment 52: 163-172. doi: 10.1016/0034-4257(95)00018-V

Kuusk, A. 1995. A fast invertible canopy reflectance model. Remote Sensing of Environment 51: 342-350. doi: 10.1016/0034-4257(94)00059-V

Keetch, J.J., and G.M. Byram. 1968. A drought index for forest fire control. USDA Forest Service Research Paper SE-38. Southeastern Forest Experiment Station, Asheville, North Carolina, USA.

Kolb, J.K., and J.S. Sperry. 1999. Differences in drought adaptation between subspecies of sagebrush (*Artemisia tridentata*). Ecology 80: 2373-2384.

Lawson, B.D., and B.C. Hawkes. 1989. Field evaluation of moisture content model for medium sized logging slash. Pages 247-257 in: D.C. MacIver, H. Auld, and R.Whitewood, editors. Proceedings of the 10th Conference on Fire and Forest Meteorology, 17-21 April 1989, Ottawa, Canada.

Le Hégarat-Mascle, S., M. Zribi, F. Alem, A. Weisse, and C. Loumagne. 2002. Soil moisture estimation from ERS/SAR data: toward an operational methodology. IEEE Transactions on Geoscience and Remote Sensing 40: 2647-2658. doi: 10.1109/TGRS.2002.806994

Littell, J.S., D. McKenzie, D.L. Peterson, and A.L. Westerling. 2009. Climate and wildfire area burned in western US.ecoprovinces, 1916-2003. Ecological Applications 19: 1003-1021. doi: 10.1890/07-1183.1

Njoku, E.G., and D. Entekhabi. 1996. Passive microwave remote sensing of soil moisture. Journal of Hydrology 184: 101-129. doi: 10.1016/0022-1694(95)02970-2

Njoku, E.G., T.J. Jackson, V. Lakshmi, T.K. Chan, and S.V. Nghiem. 2003. Soil moisture retrieval from AMSR-E. IEEE Transactions on Geoscience and Remote Sensing 41: 215-229. doi: 10.1109/TGRS.2002.808243

Pollet, J., and A. Brown. 2007. Fuel moisture sampling guide. Bureau of Land Management, Utah State Office, Salt Lake City, USA.

Riaño, D., P. Vaughan, E. Chuvieco, P.J. Zarco-Tejada, and S.L. Ustin. 2005. Estimation of fuel moisture content by inversion of radiative transfer models to simulate equivalent water thickness and dry matter content: analysis at leaf and canopy level. I EEE Transactions on Geoscience and Remote Sensing 43: 819-826. doi: 10.1109/TGRS.2005.843316

Roberts, D.A., P.E. Dennison, S. Peterson, S. Sweeney, and J. Rechel. 2006. Evaluation of Airborne Visible/Infrared Imaging Spectrometer (AVIRIS) and Moderate Resolution Imaging Spectrometer (MODIS) measures of live fuel moisture and fuel condition in a shrubland ecosystem in southern California. Journal of Geophysical Research 111, G04S02. doi: 10.1029/2005JG000113

Rothermel, R.C. 1972. A mathematical model for predicting fire spread in wildland fuels. USDA Forest Service Research Paper INT-115. Intermountain Forest and Range Experiment Station, Ogden, Utah, USA.

Rouse, J.W., R.H. Haas, J.A. Schell, and D.W. Deering. 1973. Monitoring vegetation systems in the Great Plains with ERTS. Pages 309-317 in: S.C. Freden, E.P. Mercanti, and M.A. Becker, editors. Proceedings of the Third Earth Resources Technology Satellite Symposium, SP-351 Volume I. NASA, 10-14 December 1973, Washington, D.C., USA.

Schulze, E.-D., E. Beck, and M.-H. Klaus. 2005. Water relations of plants. Pages 277-311 in: E.-D. Schulze, E. Beck, and M.-H. Klaus, editors. Plant ecology. Springer, Berlin, Germany.

Sebastián-López, A., J. San-Miguel-Ayanz, and R.E. Burgan. 2002. Integration of satellite sensor data, fuel type maps and meteorological observation for evaluation of forest fire risk at the pan-European scale. International Journal of Remote Sensing 23: 2713-2719. doi: 10.1080/01431160110107761

Serrano, L., S.L. Ustin, D.A. Roberts, J.A. Gamon, and J. Peñuelas. 2000. Deriving water content of chaparral vegetation from AVIRIS data. Remote Sensing of Environment 74: 570-581. doi: 10.1016/S0034-4257(00)00147-4

Sims, D.A., A.F. Rahman, E.F. Vermote, and Z. Jiang. 2011. Seasonal and inter-annual variation in view angle effects on MODIS vegetation indices at three forest sites. Remote Sensing of Environment 115: 3112-3120. doi: 10.1016/j.rse.2011.06.018

Snyder, R., and W. Pruitt. 1992. Evapotranspiration data management in California. Pages 128-133 in: T. Engman, editor. Irrigation and drainage: saving a threatened resource—in Search of solutions. American Society of Civil Engineers, New York, New York, USA.

Stocks, B.J., B.D. Lawson, M.E. Alexander, C.E. Van Wagner, R.S. McAlpine, T.J. Lynham, and D.E. Dubé. 1989. The Canadian Forest Fire Danger Rating System: an overview. The Forestry Chronicle 65: 258-265.

Stow, D., M. Niphadkar, and J. Kaiser. 2006. Time series of chaparral live fuel moisture maps derived from MODIS satellite data. International Journal of Wildland Fire 15: 347-360. doi: 10.1071/WF05060

Trombetti, M., D. Riaño, M. Rubio, Y. Cheng, and S. Ustin. 2008. Multi-temporal vegetation canopy water content retrieval and interpretation using artificial neural networks for the continental USA. Remote Sensing of Environment 112: 203-215. doi: 10.1016/j.rse.2007.04.013

Ustin, S.L., D.A. Roberts, J. Pinzón, S. Jacquemoud, M. Gardner, G. Scheer, C.M. Castañeda, and A. Palacios-Orueta. 1998. Estimating canopy water content of chaparral shrubs using optical methods. Remote Sensing of Environment 65: 280-291. doi: 10.1016/S0034-4257(98)00038-8

Vermote, E.F., and S. Kotchenova. 2008. Atmospheric correction for the monitoring of land surfaces. Journal of Geophysical Research 113, D23S90. doi: 10.1029/2007JD009662

Viegas, D.X., J. Pinõl, M.T. Viegas, and R. Ogaya. 2001. Estimating live fine fuels moisture content using meteorological-based indices. International Journal of Wildland Fire 10: 223-240. doi: 10.1071/WF01022

Yebra, M., and E. Chuvieco. 2009. Linking ecological information and radiative transfer models to estimate fuel moisture content in the Mediterranean region of Spain: solving the ill-posed inverse problem. Remote Sensing of Environment 113: 2403-2411. doi: 10.1016/j.rse.2009.07.001

Yebra, M., E. Chuvieco, and D. Riaño. 2008. Estimation of live fuel moisture content from MODIS images for fire risk assessment. Agricultural and Forest Meteorology 148: 523-536. doi: 10.1016/j.agrformet.2007.12.005

Zarco-Tejada, P. 2003. Water content estimation in vegetation with MODIS reflectance data and model inversion methods. Remote Sensing of Environment 85: 109-124. doi: 10.1016/S0034-4257(02)00197-9

Zribi, M., N. Baghdadi, N. Holah, and O. Fafin. 2005. New methodology for soil surface moisture estimation and its application to ENVISAT-ASAR multi-incidence data inversion. Remote Sensing of Environment 96: 485-496. doi: 10.1016/j.rse.2005.04.005